Journal of Fluorine Chemistry 135 (2012) 265–271

Contents lists available at SciVerse ScienceDirect

Journal of Fluorine Chemistry

journal homepage: www.elsevier.com/locate/fluor

Synthesis, physical–chemical properties and *in vitro* photodynamic activity against oral cancer cells of novel porphyrazines possessing fluoroalkylthio and dietherthio substituents

Jaroslaw Piskorz [a], Paulina Skupin [a], Sebastian Lijewski [b], Maciej Korpusinski [b], Mateusz Sciepura [b], Krystyna Konopka [c], Stanislaw Sobiak [b], Tomasz Goslinski [b], Jadwiga Mielcarek [a,*]

[a] Department of Inorganic and Analytical Chemistry, Poznan University of Medical Sciences, Grunwaldzka 6, 60-780 Poznan, Poland
[b] Department of Chemical Technology of Drugs, Poznan University of Medical Sciences, Grunwaldzka 6, 60-780 Poznan, Poland
[c] Department of Biomedical Sciences, University of the Pacific, Arthur A. Dugoni School of Dentistry, San Francisco, USA

ARTICLE INFO

Article history:
Received 14 November 2011
Received in revised form 5 December 2011
Accepted 9 December 2011
Available online 19 December 2011

Keywords:
Fluorinated porphyrinoids
Porphyrazine
Carcinoma
Photodynamic therapy
Singlet oxygen

ABSTRACT

Novel porphyrazines possessing fluoroalkylthio and dietherthio peripheral substituents were synthesized and tested from the peripheral substituent effects on their physical–chemical properties, including metal binding abilities and solvatochromic effects. Two porphyrazines were subjected to singlet oxygen generation measurements using 1,3-diphenylisobenzofuran as a singlet oxygen scavenger and examined *in vitro* towards oral cancer cells. Biological investigation performed on two human squamous carcinoma cell lines derived from the tongue (HSC-3) and from the buccal mucosa (H413) revealed moderate activity and selectivity of novel magnesium(II) porphyrazine possessing peripheral 4-fluorobutylthio substituents.

1. Introduction

Porphyrazines (pzs) are aromatic macrocyclic compounds consisting of four pyrrolic rings linked together with azide groups instead of methine bridges found in the naturally occurring porphyrins. Pzs can be modified in their peripheral β-positions with different groups or rings containing heteroatoms, including sulfur entities, which significantly affect their physical–chemical properties [1,2].

In the recent years porphyrazines possessing thioether groups in their β-positions have been researched for medical applications, especially photodynamic therapy of cancer (PDT) [3–7]. It was shown that the phototoxic effect of various thioether porphyrazines may be controlled by peripheral sulfur modifications with various groups, which affect their hydrophilic–lipophilic balance [5]. Photodynamic activity of some sulfur-modified porphyrazines has been evaluated on normal and cancer cell lines, including a human lung adenocarcinoma (A549), showing a decrease of the number of viable cancer cells up to 70% [3]. The relationship between the structure of thioether porphyrazines and their ability to bind liposomes and generate singlet oxygen has been found [6]. Moreover, a new poly(carbonylalkylthio)porphyrazine was synthesized and inserted into liposomes to improve the potentiality of multiple-approach cancer therapy [8]. Additionally, thioether porphyrazines have been tested as metal ion sensors due to their excellent complexation abilities and catalysts in oxidation reactions [9–12]. Thioether porphyrazines have been also applied for the preparation of the Langumir–Blodgett thin films and used as environmental gas probes [13]. Noteworthy, self-organized porphyrazine films have been developed for molecular electronics and nanotechnology [2,14,15].

It has been known that the introduction of fluorine atoms to biologically active compounds modulates their physical–chemical and pharmacological properties [16]. These alterations allow their use in many therapeutic applications, including treatment of bacterial and fungal infections, cancer, cardiovascular and central nervous system diseases [17,18]. Many porphyrinoids possessing peripheral fluorine atoms and groups containing fluorine, show potential for photodynamic therapy due to their enhanced stability, high level of singlet oxygen production, lipophilicity, and selective accumulation in tumor cells [19–21]. Additionally, it has been demonstrated that porphyrins with fluorine atoms can be applied in

* Corresponding author at: Department of Inorganic and Analytical Chemistry, Faculty of Pharmacy, Poznan University of Medical Sciences, Grunwaldzka 6, 60-780 Poznan, Poland. Tel.: +48 61 854 66 04; fax: +48 61 854 66 09.
E-mail address: jmielcar@ump.edu.pl (J. Mielcarek).

0022-1139/$ – see front matter © 2011 Elsevier B.V. All rights reserved.
doi:10.1016/j.jfluchem.2011.12.003

in vivo imaging using ^{19}F NMR [20]. Recently, we reviewed some fluorinated porphyrins, phthalocyanines, chlorines and corroles, which display potential applications in biology and medicine [22]. However, only a few examples of porphyrazines containing peripheral fluorine substituents have been reported [23,24].

This paper reports the synthesis of the series of novel porphyrazines possessing fluoroalkylthio and dietherthio peripheral substituents and their physical–chemical properties including metal binding abilities and solvatochromic effects. Additionally, two porphyrazines were examined *in vitro* towards oral cancer cells using two human squamous carcinoma cell lines derived from the tongue (HSC-3) and from the buccal mucosa (H413).

2. Results and discussion

2.1. Synthesis and characterization

New thioether porphyrazines **4**–**8** substituted with dietherthio and fluoroalkylthio groups were synthesized (Fig. 1). Alkylation reactions of dimercaptomaleonitrile disodium salt **1** with 4-fluorobutyl bromide and 2-(2-ethoxyethoxy)ethyl bromide in ethanol following Akkus and Gül procedure led to novel dinitriles **2** and **3**, respectively [25].

Novel dinitriles were used in the Linstead macrocyclization reactions using the template effect of magnesium butanolate in *n*-butanol [26,27]. Initially, the symmetrical porphyrazine **4** containing 4-fluorobutylthio peripheral substituents was synthesized starting from dinitrile **2** with 20% overall yield. Mixed macrocyclization reaction using dinitriles **2** (excess) and **3** led to the above mentioned symmetrical pz **4** in 16% overall yield, and unsymmetrical pz **5** containing peripheral 4-fluorobutylthio in excess and 2-(2-ethoxyethoxy)ethylthio groups in 14% overall yield. Similarly, mixed macrocyclization reaction using dinitriles **2** and **3** (excess) led to the symmetrical pz **6** containing 2-(2-ethoxyethoxy)ethylthio groups in 17% and mixed pz **7** possessing peripheral dietherthio in excess and 4-fluorobutylthio substituents in 13% yield. Pz **6** was further treated with trifluoroacetic acid to give the metal-free porphyrazine **8** in 53% overall yield.

Porphyrazines **4**–**8** were characterized spectroscopically using ^{1}H NMR, ^{13}C NMR and ^{19}F NMR (fluorine containing compounds), UV–vis and MS MALDI. Other NMR techniques (^{1}H–^{1}H COSY, ^{1}H–^{1}H NOESY, HSQC, HMBC) were used to fully characterize mixed porphyrazines **5** and **7** (see supplementary). The structures of pzs **4**–**8** were widely discussed and included into the supplementary.

2.2. Metal binding ability

The ability of the new magnesium porphyrazines **4**–**7** to coordinate metal cations was evaluated by monitoring the UV–vis spectral changes during titrations with *bis*(benzonitrile)palladium(II) chloride (Fig. 2).

Titration of symmetrical pz **4** endowed with 4-fluorobutylthio groups resulted in a gradual decrease of the Q-band with the maximum absorption at 668 nm that continued until a Pd^{2+}–ligand ratio of 1 equivalent was reached. Thereafter, a new blue-shifted band at 644 nm appeared when Pd^{2+}–ligand ratio reached values 3 and 10. Another change was observed in the Soret band placed at 375 nm. An increase of the palladium(II) ion concentration to values higher than 0.5 equivalent resulted in a decrease and a shift of this band to the longer wavelength (380–390 nm). Moreover, the diffused broad band at about 500 nm disappeared when Pd^{2+}–porphyrazine ratio reached 1 equivalent.

The UV–vis spectra of mixed pz **5** possessing an excess of 4-fluorobutylthio groups, titrated with palladium(II) ions revealed similar changes. Absorption of the Q-band at 669 nm decreased when Pd^{2+}–ligand ratio of 1 was reached. A new band appeared at 643 nm when palladium(II)–porphyrazine ratio was higher than 2. The asymmetrically split Soret band with absorption maximum at 375 nm decreased and transformed into broad, split band possessing absorption maxima at 341 nm and 387 nm that continued until Pd^{2+}–ligand ratio reached 3. Higher concentrations of Pd^{2+}–ligand ratio (up to 10) caused disappearance of the high energetic sub-band and the shift of the Soret band to 381 nm. Moreover, a characteristic band at 500 nm disappeared when Pd^{2+}–ligand ratio reached 1.

Titration of mixed pz **7** endowed with a majority of 2-(2-ethoxyethoxy)ethylthio groups resulted in a decrease of the Q-band at 669 nm and a parallel increase of a new band at 643 nm. The Soret band shifted from 375 nm to 380–385 nm

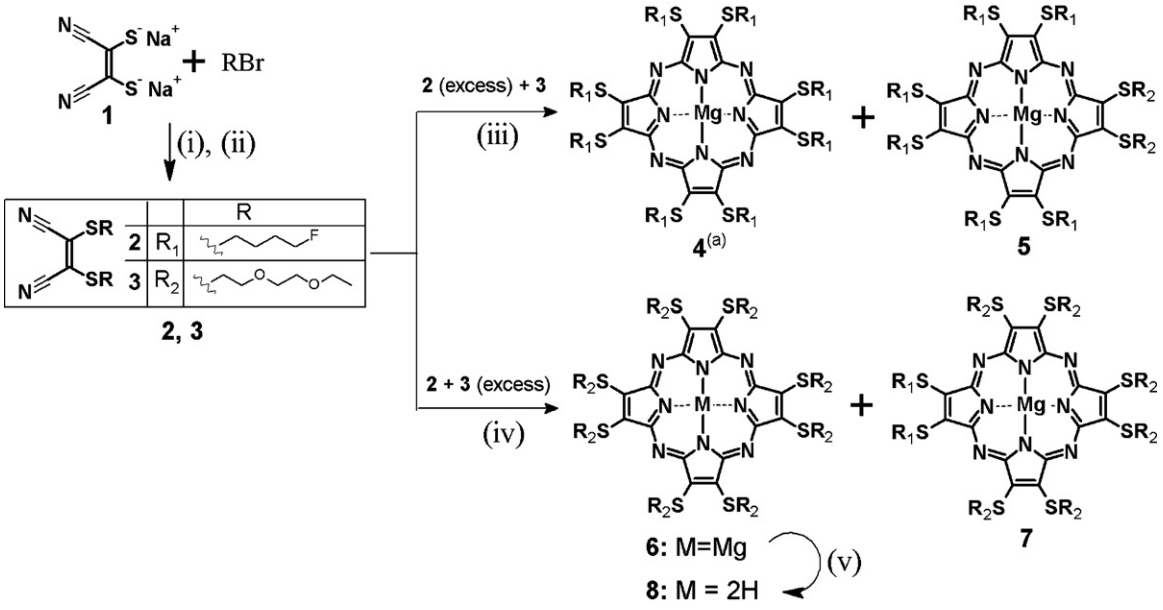

Fig. 1. Reagents and conditions: (i) $Br(CH_2)_3CH_2F$, EtOH, r.t., 72 h (79%); (ii) $Br(CH_2CH_2O)_2CH_2CH_3$, r.t., 72 h (86%); (iii) $Mg(OC_4H_9)_2$, *n*-BuOH, reflux, 16 h (**4** – 16%, **5** – 14%); (iv) $Mg(OC_4H_9)_2$, *n*-BuOH, reflux, 16 h (**6** – 19%, **7** – 13%); (v) CF_3COOH, 20 min (**8** – 53%); (a) **4** was also obtained separately: $Mg(OC_4H_9)_2$, *n*-BuOH, reflux, 20 h (20%).

until Pd^{2+}–ligand ratio of 2 was reached. Additionally, a band at 500 nm disappeared when palladium(II) ion equivalents reached 1.

Titration of symmetrical pz **6** possessing 2-(2-ethoxyethoxy)ethylthio groups with Pd^{2+} cations, revealed three characteristic changes in UV–vis spectra, as well. The Q-band and the Soret band shifted from 670 nm to 643 nm and 376 nm to 381 nm, respectively. Finally, the band at 500 nm disappeared when Pd^{2+}–ligand ratio reached the value of 1, similarly to that observed for earlier described pzs.

The changes noticed in the UV–vis spectra for all titrated compounds reveal some tendencies. The shift of the Q-band from 668–670 nm to 643–644 nm was observed for all pzs regardless of peripheral substituents, which indicated a key role of sulfur atoms present in pzs β-positions for metal binding ability. Changes in the absorption maxima of the Soret band from the range 375–376 nm to 380–390 nm revealed that nitrogen *meso* atoms are engaged in the binding of the palladium(II) ions, as well. The small, flattened band at about 500 nm is a result of $n \rightarrow \pi^*$ donation of a lone pair of electrons from sulfur atoms to the macrocycle ring. According to Michel at al. [27], the disappearance of the band $n \rightarrow \pi^*$ is a result of the interaction between a lone pair of electrons present on sulfur atoms and palladium(II) cations. These observations are also consistent with the data obtained for thioether porphyrazines titrated with palladium(II) cations [28,29] and other metal ions [27,30].

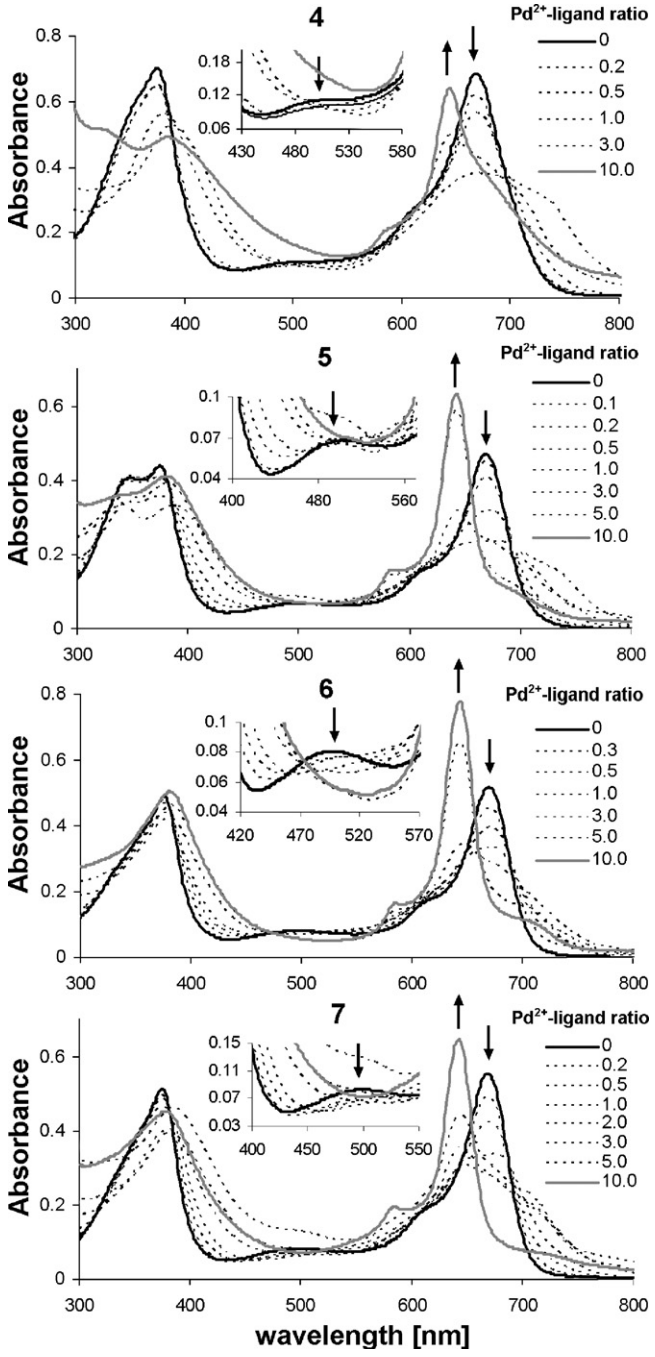

Fig. 2. Changes in the UV–vis spectra of pzs **4**–**7** titrated with $PdCl_2(PhCN)_2$ in dichloromethane/methanol (1:1, v/v). Variations of the band ~500 nm (inset).

2.3. Solvatochromic effects

Solvatochromic effects of pzs **4**–**7** were evaluated by monitoring the changes in the UV–vis spectra. In the recorded absorption spectra two characteristic bands, a broad intense Soret band in the range of 360–390 nm and an intense Q-band at 664–673 nm were observed. Moreover, the Soret band of pz **5** was asymmetrically split with absorption maxima at 340–344 nm and 374–380 nm. The positions and intensities of the Q-bands within the pzs tested were affected by the type of solvent used (see Fig. 6S, supplementary). It was found that Q-bands were significantly red shifted when pyridine, toluene or dichloromethane were used as solvents. The Q-band red shift was the most significant for symmetrical pzs **4** and **6** in toluene. For mixed pzs **5** and **7** the most significant Q-band red shift was observed in pyridine. The most blue shifted Q-band was observed for all porphyrazines investigated when acetonitrile was used as the solvent.

The relations between Q-band shift (λ_{max}) of porphyrazines **4**–**7** and $1/F$ value or dipole moment (μ) of the solvent were determined to evaluate the solvatochromic effects according to the procedures [31,32]. The $1/F$ value is a rational function of the solvent's refractive index (n), calculated from the Bayliss equation $F = (n^2 - 1)/(2n^2 + 1)$. The wavelength of maximum absorbance for the pzs tested and value characteristic for the solvents used ($1/F$, μ) are presented in Table 1. Correlation indices (r^2) characterizing the relationships between Q-band shift of pzs **4**–**7** and dipole moment or $1/F$ value of solvents and selected plots are collected in Fig. 7S, supplementary.

Summarizing, the linear correlation between Q-band shifts and $1/F$ values suggests that changes observed in the electronic absorption spectra have been mainly a result of solvation rather than coordination processes, and there is no correlation between the coordinating strength of the solvent and the red shift [31]. Therefore, solvation processes dominate for mixed pz **5** which exhibited correlation between Q-band shifts and $1/F$ values, with r^2

Table 1
UV–vis spectral data of **4**–**7** in various organic solvents (dipole moments and refractive indices) [31,33].

Solvent	$1/F$	Dipole moment [D]	Q-band λ_{max} [nm]			
			4	**5**	**6**	**7**
Pyridine	4.34	2.21	667	673	668	672
Toluene	4.42	0.37	669	672	671	670
Dichloromethane	4.76	1.60	668	671	669	668
Tetrahydrofuran	5.52	1.75	667	669	668	670
Ethyl acetate	5.40	1.78	664	668	668	668
Ethanol	5.52	1.69	667	668	667	666
Acetonitrile	5.72	3.92	664	665	665	664
Methanol	5.93	1.70	667	667	667	667

$F = (n^2 - 1)/(2n^2 + 1)$; n, refractive index of the solvent

of 0.90 for 8 solvents. Nevertheless, other processes connected with dipole moments and coordinating strength of the solvents might prevail over solvation for porphyrazines **4** and **6** with r^2 of 0.94 for 7 solvents and 0.80 for 8 solvents, respectively.

2.4. Singlet oxygen generation

The most stable porphyrazines **4** and **8** were subjected to photochemical study. The quantum yields of singlet oxygen generation were evaluated using a photooxidation reaction of 1,3-diphenylisobenzofuran. Solutions of **4**, **8** and a reference zinc(II) phthalocyanine irradiated with a light of specific wavelength undergo activation and interact with oxygen (ground state) producing singlet oxygen. Upon interaction with singlet oxygen, DPBF is oxidized and decomposed which is manifested in the UV–vis spectrum as a decrease in the absorbance at 417 nm (Fig. 3) [34–36]. The measurements for **4**, **8** and ZnPc were performed in DMF. In DMSO an additional red shifted band in the Q-band region appeared, suggesting the H-type aggregates formation and thus slowing down the oxidation of DPBF [37].

Changes in the Q-band intensity of pzs **4** and **8** after 60 min of irradiation were small (did not exceed 3%), which indicates their good stability and resistance to photobleaching. However, this experiment revealed their low activity to generate singlet oxygen. The singlet oxygen quantum yields (Φ_Δ) for pzs **4** and **8** were found to be low – 0.024 and 0.022, respectively, as compared to that measured for ZnPc ($\Phi_\Delta = 0.56$) [38].

2.5. Photodynamic activity in vitro

The photodynamic activity of porphyrazines **4** and **8** was examined *in vitro* using two human OSCC cell lines, HSC-3 cells derived from the tongue and H413 cells from the buccal mucosa. To determine dark toxicity, the cells were incubated with pzs **4** or **8**, at concentrations of 1, 5, 10 and 50 μmol, in serum free medium for 24 h at 37 °C. At these concentrations both porphyrazines did not reduce the viability of HSC-3 and H413 cells (see Table 3S, supplementary). Aggregation observed at 50 μM did not result in the loss of cell viability. Analysis of light-induced toxicity of pzs **4** and **8** in HSC-3 and H413 cells is shown in Fig. 4.

The cells were incubated with pz **4** or **8** (1 and 5 μmol) for 24 h and subsequently exposed to light (600–850 nm) for 20 min at a distance of 10 cm from the light source. HSC-3 and H413 cells were incubated with pzs **4** and **8** for 24 h in serum-free medium. Cell viability was quantified by the Alamar Blue assay. Results are expressed as the percentage of control cells incubated with medium/0.5% DMSO alone. Data represent the mean values obtained from triplicate wells. At both concentrations, pz **4** decreased the viability of H413 cells by 30–35% (see Table 4S, supplementary). Interestingly, no light-induced toxicity was observed for HSC-3 cells treated with pz **4**. Pz **8** did not show any phototoxic effect both in HSC-3 and H413 cells. Thus, the photodynamic effect of pz **4** appears to be cell dependent, despite the fact that these cells are derived from the same type of tumor (OSCC).

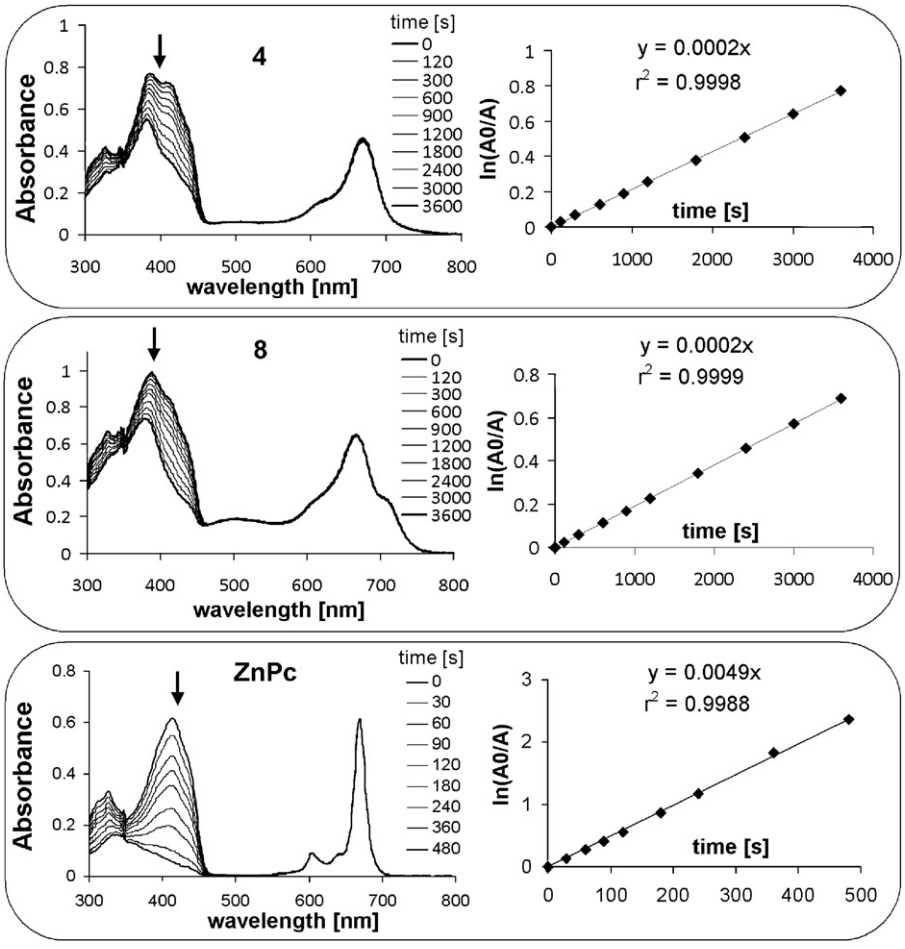

Fig. 3. Changes in the UV–vis spectra for DPBF and photosensitizers (**4**, **8**, ZnPc) in DMF and correlations between $\ln(A_0/A)$ and irradiation time; ZnPc–zinc(II) phthalocyanine.

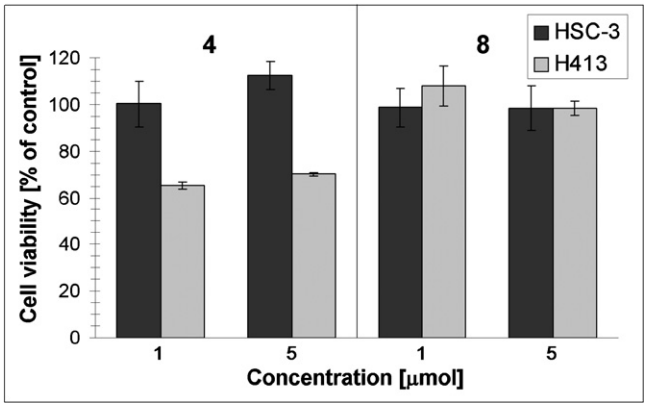

Fig. 4. Light-dependent toxicity of pzs **4** and **8** in HSC-3 and H413 cells. The cells were incubated with 1 and 5 μmol of pz **4** or **8** in serum-free medium for 24 h. Cell viability was quantified by the Alamar Blue assay. Results are expressed as the percentage of viability of control cells exposed to light in the absence of photosensitizers. Data represent the mean ± standard deviation (SD) obtained from two independent experiments performed in triplicate.

Dark and light toxicity of six peripherally functionalized porphyrazines have been investigated recently in nine human tumor-derived cell lines (five OSCC, three breast adenocarcinoma, one lung adenocarcinoma) and in one non-tumor derived, SV40 transfected fibroblast-like human embryonic cell line [7]. Interestingly, therein described demetallated thioether porphyrazine, which is an analog of pz **8**, does not exhibit dark and photo-induced toxicity in tumor cells. Therefore, it appears that the moderate phototoxicity of pz **4** observed in our study with H413 cells may be caused by a novel 4-fluorobutylthio periphery. Future work should more closely examine the mechanism, by which pz **4** caused the light-induced cell death as well as the cell type dependency of light-induced toxicity.

3. Conclusions

Novel porphyrazines possessing fluoroalkylthio and diethertho peripheral substituents were synthesized following an established Linstead macrocyclization procedure and characterized using MS MALDI and various NMR techniques including ^{1}H, ^{13}C and ^{19}F NMR. A detailed discussion of the structure was included.

Compounds were tested from the peripheral substituent effects on their photochemical properties, including metal binding abilities and solvatochromic effects. Summarizing, the linear correlation between Q-band shifts and 1/*F* values suggests that changes observed in electronic absorption spectra are mainly a result of solvation rather than coordination processes, and there is no correlation between the coordinating strength of the solvent and the observed Q-band red shift. Two porphyrazines were subjected to the singlet oxygen generation measurements using DPBF as a singlet oxygen scavenger and examined *in vitro* towards oral cancer cells. The singlet oxygen quantum yields (Φ_{Δ}) were found to be lower than that measured for the referenced zinc(II) phthalocyanine.

Biological investigation performed on two human squamous carcinoma cell lines derived from the tongue (HSC-3) and from the buccal mucosa (H413) revealed moderate activity and selectivity of magnesium(II) porphyrazine possessing peripheral 4-fluorobutylthio substituents. This pz decreased the viability of H413 cells by 30–35%. Noteworthy, no light-induced toxicity was observed for HSC-3 cells treated with examined porphyrazines. The observed cell-depended activity of magnesium(II) porphyrazine possessing 4-fluorobutylthio substituents seems to be interesting as both cancer cell lines are derived from the same type of tumor (OSCC) and thus worth further examination.

4. Experimental

4.1. Synthesis

4.1.1. 2,3-Bis(4-fluorobutylthio)maleonitrile (2)

1-Bromo-4-fluorobutane (1.076 μL, 10.00 mmol) was added dropwise to dimercaptomaleonitrile disodium salt (**1**, 745 mg, 4.00 mmol) in anhydrous ethanol (20 mL) during 30 min and stirred at room temperature for another 66 h. After the solvent was evaporated, the residual oil was chromatographed (*n*-hexane/ethyl acetate, 7:1 to 7:3, v/v) to give **2** as yellow oil (921 mg, 79%): R_f (*n*-hexane/ethyl acetate, 7:5, v/v) = 0.72. ^{1}H NMR (400 MHz, $CDCl_3$): δ 4.48 (dt, 4H, $^{2}J_{H-F}$ = 47 Hz, ^{3}J = 5 Hz, 2× CH_2F), 3.17 (t, 4H, ^{3}J = 7 Hz, 2× SCH_2), 1.87 (m, 4H, 2× $SCH_2\underline{CH_2}$), 1.92–1.76 (overlapped, 4H, 2× $\underline{CH_2}CH_2F$). ^{13}C NMR (100 MHz, $CDCl_3$): δ 121.0, 111.9, 83.1 (d, $^{1}J_{C-F}$ = 165 Hz, CH_2F), 34.5 (SCH_2), 29.0 (d, $^{2}J_{C-F}$ = 20 Hz, $\underline{CH_2}CH_2F$), 26.1 (d, $^{3}J_{C-F}$ = 4 Hz, $SCH_2\underline{CH_2}$). ^{19}F NMR (376 MHz, $CDCl_3$): δ −142.9 (m). MS (ES): *m*/*z* 291 $[M+H]^+$, 271 $[M-F]^+$, 215 $[M-(CH_2)_3CH_2F]^-$. Anal. Calcd. for $C_{12}H_{16}F_2N_2S_2$: C, 49.63; H, 5.55; N, 9.63; S, 22.08. Found: C, 49.69; H, 5.86; N, 9.82; S, 21.91.

4.1.2. 2,3-Bis[2-(2-ethoxyethoxy)ethylthio]maleonitrile (3)

2-(2-Ethoxyethoxy)ethyl bromide (1.00 mL, 6.68 mmol) dissolved in 1 mL of ethanol was added to dimercaptomaleonitrile disodium salt (**1**, 500 mg, 2.69 mmol) in anhydrous ethanol (20 mL) and stirred at room temperature for another 72 h. After the solvent was evaporated, the residual oil was chromatographed (*n*-hexane/ethyl acetate, 7:5, v/v) to give **3** as yellow oil (869 mg, 86%): R_f (*n*-hexane/ethyl acetate, 7:5, v/v) = 0.36. ^{1}H NMR (400 MHz, $CDCl_3$): δ 3.76 (t, 4H, ^{3}J = 6 Hz), 3.64 (m, 4H), 3.58 (m, 4H), 3.52 (q, 4H, ^{3}J = 7 Hz, 2× $\underline{CH_2}CH_3$), 3.32 (t, 4H, ^{3}J = 6 Hz), 1.21 (t, 6H, ^{3}J = 7 Hz, 2× CH_3). ^{13}C NMR (100 MHz, $CDCl_3$): δ 121.2, 112.1, 70.7, 69.7, 69.5, 66.7, 34.8, 15.1. MS (ES): *m*/*z* 397 $[M+Na]^+$. Anal. Calcd. for $C_{16}H_{26}N_2O_4S_2$: C, 51.31; H, 7.00; N, 7.48; S, 17.12. Found: C, 51.26; H, 7.22; N, 7.55; S, 17.16.

4.1.3. 2,3,7,8,12,13,17,18-Octakis-(4-fluorobutylthio) porphyrazinatomagnesium(II) (4)

Magnesium turnings (13 mg, 0.55 mmol), small crystal of iodine and *n*-butanol (8 mL) were refluxed for 7 h. After the mixture was cooled to room temperature, dinitrile **2** (160 mg, 0.55 mmol) was added and the reaction mixture was refluxed for another 20 h. After, the solvent was evaporated with toluene, the residual solid was dissolved in dichloromethane, Celite filtered and chromatographed (*n*-hexane/ethyl acetate, 7:1 to 7:3, v/v) to give blue porphyrazine **4** (32 mg, 20%): R_f (*n*-hexane/ethyl acetate, 7:5, v/v) = 0.66. UV–vis (dichloromethane/methanol, 1:1, v/v): λ_{max}, nm (log ε) = 375 (4.59), 668 (4.57). ^{1}H NMR (400 MHz, d_5-pyridine): δ 4.51 (dt, 16H, $^{2}J_{H-F}$ = 48 Hz, ^{3}J = 6 Hz, 8× CH_2F), 4.36 (m, 16H, 8× SCH_2), 2.09 (m, 16H, 8× $SCH_2\underline{CH_2}$), 2.05–1.85 (overlapped, 16H, 8× $\underline{CH_2}CH_2F$). ^{13}C NMR (100 MHz, d_5-pyridine): δ 157.4, 140.5, 84.0 (d, $^{1}J_{C-F}$ = 163 Hz, 8× CH_2F), 35.2 (8× SCH_2), 30.1 (d, $^{2}J_{C-F}$ = 19 Hz, 8× $\underline{CH_2}CH_2F$), 26.7 (d, $^{3}J_{C-F}$ = 5 Hz, 8× $SCH_2\underline{CH_2}$). ^{19}F NMR (376 MHz, $CDCl_3$): δ −141.6 (m). MS (MALDI) *m*/*z* 1185 $[M+H]^+$.

4.1.4. Pz 4 and 2,3-bis-[2-(2-ethoxyethoxy)ethylthio]-7,8,12,13,17,18-hexakis-(4-fluorobutylthio)porphyrazinatomagnesium(II) (5)

Magnesium turnings (56.0 mg, 2.33 mmol), small crystal of iodine and *n*-butanol (15 mL) were refluxed for 4 h. After the mixture was cooled to room temperature, dinitrile **2** (580 mg, 2.00 mmol) dissolved in 1 mL of *n*-butanol and dinitrile **3** (116 mg, 0.31 mmol) in 1 mL of *n*-butanol were added and the reaction mixture was refluxed for another 16 h. Then the solvent was evaporated with toluene and the residual solid was dissolved in

dichloromethane, Celite filtered and chromatographed (*n*-hexane/ethyl acetate, 7:3 to 2:3, v/v). After extensive column chromatography two porphyrazines were separated: symmetrical pz **4** (92 mg, 16%) and mixed pz **5** (54 mg, 14%).

5: R_f (*n*-hexane/ethyl acetate, 7:5, v/v) = 0.10. UV–vis (dichloromethane/methanol, 1:1, v/v): λ_{max}, nm (log ε) = 669 (4.81), 375 (4.80). ^{1}H NMR (400 MHz, d_5-pyridine) δ 4.60 (m, overlapped, 4H, 2× S$\underline{CH_2}CH_2O$), 4.51 (dm, 12H, $^2J_{H-F}$ = 48 Hz, 6× CH_2F), 4.40–4.30 (m, overlapped, 12H, 6× SCH_2), 4.18 (t, 4H, ^3J = 6 Hz, 2× $SCH_2\underline{CH_2}O$), 3.73 (t, 4H, ^3J = 5 Hz, 2× $SCH_2CH_2O\underline{CH_2}$), 3.54 (m, 4H, 2× $SCH_2CH_2OCH_2\underline{CH_2}$), 3.34 (q, 4H, ^3J = 7 Hz, 2× $\underline{CH_2}CH_3$), 2.09 (bs, 24H, 6× $\underline{CH_2CH_2}CH_2F$), 1.02 (t, 6H, ^3J = 7 Hz, 2× CH_3). ^{13}C NMR (100 MHz, d_5-pyridine) δ 157.4, 140.7, 84.0 (d, $^1J_{C-F}$ = 164 Hz, 8× CH_2F), 71.4, 70.8, 70.2, 66.5, 35.5, 35.1, 30.1 (d, $^2J_{C-F}$ = 19 Hz, 8× $\underline{CH_2}CH_2F$), 26.6, 15.4. ^{19}F NMR (376 MHz, $CDCl_3$): δ −141.8 (m). MS (MALDI) *m*/*z* 1271 $[M+H]^+$.

4.1.5. 2,3,7,8,12,13,17,18-Octakis-[2-(2-ethoxyethoxy)ethylthio]porphyrazinatomagnesium(II) (6) and 2,3,7,8,12,13-hexakis-[2(-2-ethoxyethoxy)ethylthio]-17,18-bis-(4-fluorobutylthio)porphyrazinatomagnesium(II) (7)

Magnesium turnings (56 mg, 2.33 mmol), small crystal of iodine and *n*-butanol (15 mL) were refluxed for 4.5 h. After the mixture was cooled to room temperature, dinitrile **3** (697 mg, 1.86 mmol) and dinitrile **2** (96 mg, 0.33 mmol) were added and the reaction mixture was refluxed for another 16 h. The solvent was evaporated with toluene and the residual mixture was dissolved in dichloromethane, Celite filtered, and chromatographed (dichloromethane/methanol, 50:1 to 10:1, v/v). After extensive column chromatography two porphyrazines were separated: symmetrical pz **6** (132 mg, 19%) and mixed pz **7** (60 mg, 13%).

6: R_f (dichloromethane/methanol, 4:1, v/v) = 0.88. UV–vis (dichloromethane/methanol, 1:1, v/v): λ_{max}, nm (log ε) = 375 (4.90), 669 (4.91). ^{1}H NMR (400 MHz, d_5-pyridine): δ 4.61 (t, 16H, ^3J = 6 Hz, 8× SCH_2), 4.20 (t, 16H, ^3J = 6 Hz, 8× $SCH_2\underline{CH_2}$), 3.74 (t, 16H, ^3J = 5 Hz, 8× $SCH_2CH_2O\underline{CH_2}$), 3.55 (t, 16H, ^3J = 5 Hz, 8× $SCH_2CH_2OCH_2\underline{CH_2}$), 3.36 (q, 16H, ^3J = 7 Hz, 8× $\underline{CH_2}CH_3$), 1.04 (t, 24H, ^3J = 7 Hz, 8× CH_3). ^{13}C NMR (100 MHz, d_5-pyridine): δ 157.7, 141.0, 71.5, 70.9, 70.2, 66.5, 35.4, 15.4. MS (MALDI) *m*/*z* 1521 $[M+H]^+$.

7: R_f (dichloromethane/methanol, 10:1, v/v) = 0.30. UV–vis (dichloromethane/methanol, 1:1, v/v): λ_{max}, nm (log ε) = 375 (4.83), 669 (4.86). ^{1}H NMR (400 MHz, d_5-pyridine) δ 4.59 (m, 12H, 6× S$\underline{CH_2}CH_2O$), 4.54 (dm, overlapped, 4H, $^2J_{H-F}$ = 48 Hz, 2× CH_2F), 4.35–4.25 (m, 4H, 2× SCH_2), 4.19 (m, 12H, 2× $SCH_2\underline{CH_2}O$), 3.75 (m, 12H, 6× $SCH_2CH_2O\underline{CH_2}$), 3.55 (m, 12H, 6× $SCH_2CH_2OCH_2\underline{CH_2}$), 3.36 (m, 12H, 6× $\underline{CH_2}CH_3$), 2.10 (bs, 8H, 2× $\underline{CH_2CH_2}CH_2F$), 1.04 (m, 18H, 2× CH_3). ^{13}C NMR (100 MHz, d_5-pyridine) δ 157.4, 140.6, 84.0 (d, $^1J_{C-F}$ = 163 Hz, 2× CH_2F), 71.5, 70.8, 70.2, 66.5, 35.5, 35.1, 30.1 (d, $^2J_{C-F}$ = 19 Hz, 2× $\underline{CH_2}CH_2F$), 26.6 (2× $SCH_2\underline{CH_2}$) 15.4. ^{19}F NMR (376 MHz, d_5-pyridine): δ −140.2 (m). MS (MALDI) *m*/*z* 1439 $[M+H]^+$, 1437 $[M-H]^-$.

4.1.6. 2,3,7,8,12,13,17,18-Octakis-[2-(2-ethoxyethoxy)ethylthio]porphyrazine (8)

Porphyrazine **6** (110 mg, 0.072 mmol) was dissolved in trifluoroacetic acid (5 mL) and stirred in the dark for 20 min. Next the reaction mixture was poured into water-crushed ice, neutralized with saturated solution of sodium bicarbonate (150 mL) and extracted with dichloromethane (total amount 200 mL). The organic layer was evaporated to dryness and chromatographed (dichloromethane/methanol, 50:1, v/v) to give **8** (57 mg, 53%): R_f (dichloromethane/methanol, 20:1, v/v) = 0.80. UV–vis (dichloromethane/methanol, 1:1, v/v): λ_{max}, nm (log ε) = 360 (4.31), 639 (4.07) 708 (4.22). ^{1}H NMR (400 MHz, d_5-pyridine): δ 4.60 (t, 16H, ^3J = 6 Hz, 8× SCH_2), 4.23 (t, 16H, ^3J = 6 Hz, 8× $SCH_2\underline{CH_2}$), 3.76 (t, 16H, ^3J = 5 Hz, 8× $SCH_2CH_2O\underline{CH_2}$), 3.54 (t, 16H, ^3J = 5 Hz, 8× $SCH_2CH_2OCH_2\underline{CH_2}$), 3.33 (q, 16H, ^3J = 7 Hz, 8× $\underline{CH_2}CH_3$), 1.01 (t, 24H, ^3J = 7 Hz, 8× CH_3), −1.43 (s, 2H, 2× NH). ^{13}C NMR (100 MHz, d_5-pyridine): δ 140.8, 71.3, 70.9, 70.2, 66.5, 35.4, 15.4. MS (MALDI) *m*/*z* 1500 $[M+H]^+$, 1498 $[M-H]^-$.

4.2. Spectroscopic and metallation studies

Solvatochromic effects of pzs were evaluated by monitoring the changes in the UV–vis spectra following procedure given by Beall et al. [39]. All solvents were obtained from commercial suppliers and used without further purification with the exception of ethyl acetate, methanol, ethanol, toluene, pyridine, dichloromethane, which were distilled prior to measurements. UV–vis spectra were recorded in the range of 300–900 nm. Titrations of the porphyrazines with *bis*(benzonitrile)palladium(II) chloride complex ($PdCl_2(C_6H_5CN)_2$) were used to evaluate their ability to coordinate metal cations. The UV–vis titrations were performed in dichloromethane/methanol solutions (1:1, v/v) using increasing concentrations (0.1–10 molar equivalent) of $PdCl_2(C_6H_5CN)_2$. Blank UV–vis spectra (in the absence of metal salt) were recorded for porphyrazines **4**–**7** to determine any solvent effects and they were also treated as references. Blank UV–vis spectrum of metal salt (in the absence of porphyrazines) was also recorded to make sure that there was no significant absorbance in the window of interest (300–900 nm).

4.3. Singlet oxygen generation

The quantum yields of singlet oxygen photogeneration were determined in DMF solutions (3.0 mL, no oxygen bubbled) using the relative method with zinc(II) phthalocyanine (ZnPc, Sigma–Aldrich) as a reference and 1,3-diphenylisobenzofuran (DPBF) as a chemical quencher for singlet oxygen, following recently presented methodologies [34–36]. Solutions of **4**, **8** and ZnPc in DMF with DPBF were irradiated in a 1 cm path length quartz cell with monochromatic light by a 150 W high-pressure Xe lamp (Optel) through a monochromator M250/1200/U. The irradiation wavelength was adjusted to the maximum of the absorption peak at the Q-band characteristic of each compound (sensitizer absorbance ~ 0.5). To avoid chain reactions induced by DPBF in the presence of singlet oxygen, the concentration of DPBF was set at ~3×10^{-5} mol L^{-1} and was kept the same for both the standard and the samples [40]. UV–vis spectra were recorded on a Shimadzu UV-160A spectrophotometer with PC 160 PLUS manual. The light intensity was set to 0.5 mW/cm^2 (Radiometer RD 0.2/2 with TD probe, Optel). All the experiments were performed in the dark at ambient temperature.

Zinc(II) phthalocyanine in DMF (Φ_Δ = 0.56) [38], was the reference. The singlet oxygen quantum yields were calculated by a direct comparison of the slopes in the linear region of the plots obtained for the sensitizers and the corresponding slopes obtained for the reference [36].

4.4. In vitro photodynamic activity

4.4.1. Cell cultures

Two human oral squamous cell carcinoma (OSCC) cell lines were utilized in this study. HSC-3 cells, derived from SCCs of the tongue [41] were provided by Dr. R. Kramer (University of California, San Francisco, UCSF, USA). H413 cells, derived from SCC of the buccal mucosa [42] were obtained from Dr. R. Jordan (UCSF). HSC-3 cells were cultured in Dulbecco's modified Eagle's MEM (DMEM) medium supplemented with 10% (v/v) heat-inactivated fetal bovine serum (FBS), penicillin (100 U/mL), streptomycin (100 μg/mL) and L-glutamine (4 mmol) (DMEM/10). H413 cells were maintained in DMEM/10 supplemented with Ham's Nutrient

Mixture F12 (DMEM/10/F12). Cells were incubated in tissue culture flasks (Falcon, Becton Dickinson Labware, UK) at 37 °C in a humidified atmosphere containing 5% CO_2, and were passaged 1:6 twice a week using Trypsin–EDTA solution. All media, with or without phenol red, penicillin–streptomycin solution, L-glutamine, FBS, Trypsin–EDTA, phosphate buffered saline (PBS), Dulbecco's phosphate buffered saline (DPBS), were obtained from the UCSF Cell Culture Facility, San Francisco, CA, USA. Photosensitizers were solubilized in dimethyl sulfoxide (DMSO, Sigma–Aldrich, St. Louis, MO, USA) to a final concentration of 10 mmol, and subsequently diluted in DMEM or DMEM/F12 (without FBS and phenol red) to a concentration of 50 μmol. The 50 μmol solutions were diluted in the appropriate media to obtain the desirable concentration of photosensitizer used in experiments.

4.4.2. Dark toxicity

One day before the experiment, HSC-3 and H413 cells were seeded in 48-well plates (BD Falcon™, Franklin Lakes, NJ, USA) at a density 1.8×10^5 and 1.4×10^5 cells per well, respectively, in 1 mL of complete medium (with FBS and phenol red), and used at approximately 80% confluence. Subsequently, cells were pre-washed twice with PBS (0.5 mL) and 1 mL of medium without FBS and phenol red, containing photosensitizer at a given concentration, was added to each well except controls. The FBS-free media were used to avoid binding of photosensitizers to serum proteins. After the 24 h incubation at 37 °C, cells were washed twice with PBS and 1 mL of complete medium was added to each well. Subsequently cells were incubated for 24 h at 37 °C. Cell viability was quantified by the Alamar Blue assay. Cells incubated either with medium alone or medium/0.5% DMSO served as controls.

4.4.3. Light-dependent toxicity

One day before the experiment, HSC-3 and H413 cells were seeded in 48-well plates at a density 1.8×10^5 and 1.4×10^5 cells per well, respectively, in 1 mL of complete medium, and used at approximately 80% confluence. Cells were pre-washed twice with PBS, and 1 mL of medium without FBS and phenol red, containing 1.0 or 10.0 μmol of a given photosensitizer, was added to each well except controls. The cells were incubated for 24 h at 37 °C, washed twice with PBS and then 0.5 mL of medium without FBS and phenol red was added. Subsequently, the cells were exposed to light (600–850 nm, 550 lux) from the light bulb (Dura Max 75W Med 120V A19 Cl/LL 20W, Philips Electronics North America Corporation, Andover, MA), at a distance of 10 cm from the light bulb to the plate, for 20 min. The total spectral irradiance at the level of cells, and in the presence of a water filter, was measured using a luxometer TES 1335 (TES Electrical Electronic Corp.). Infrared radiation was minimized using a 2 cm water filter between the cell plates and the light source. One plate from each experiment was not exposed to light and served as a control. Directly after light exposure, medium without FBS and phenol red was replaced with 1 mL of complete medium, and cells were incubated for 24 h at 37 °C. Cell viability was quantified by the Alamar Blue assay.

4.4.4. Cell viability

Cell morphology was evaluated by inverted phase contrast microscopy at 25× magnification. The number of viable cells used for the experiments was determined by the Trypan Blue exclusion assay (Gibco-Invitrogen Corporation, Carlsbad, CA, USA). Cell viability was quantified by the modified Alamar Blue assay [43,44]. Briefly, 1.0 mL of 10% (v/v) Alamar Blue dye in the appropriate complete medium was added to each well. After incubation at 37 °C for 2–3 h, 200 μL of the supernatant was assayed by measuring the absorbance at 570 nm and 600 nm. Cell viability (as a percentage of control cells) was calculated according to the formula $[(A_{570} - A_{600})$ of test cells$] \times 100/[(A_{570} - A_{600})$ of control cells$]$.

Acknowledgements

This study was supported by the Student Research Grants SBN in years 2008–2011 from Poznan University of Medical Sciences. The authors thank Beata Kwiatkowska and Michael Yee for excellent technical assistance.

Appendix A. Supplementary data

Supplementary data associated with this article can be found, in the online version, at doi:10.1016/j.jfluchem.2011.12.003.

References

[1] M.S. Rodriguez-Morgade, P.A. Stuzhin, J. Porphyrins Phthalocyanines 8 (2004) 1129–1165.
[2] M.J. Fuchter, C. Zhong, H. Zong, B.M. Hoffman, A.G.M. Barrett, Aust. J. Chem. 61 (2008) 235–255.
[3] N.D. Hammer, S. Lee, B.J. Vesper, K.M. Elseth, B.M. Hoffman, A.G.M. Barrett, J.A. Radosevich, J. Med. Chem. 48 (2005) 8125–8133.
[4] N. Kemikli, R. Öztürk, Inorg. Chem. Commun. 11 (2008) 338–340.
[5] B.J. Vesper, S. Lee, N.D. Hammer, K.M. Elseth, A.G.M. Barrett, B.M. Hoffman, J.A. Radosevich, J. Photochem. Photobiol. B 82 (2006) 180–186.
[6] A. Sholto, S. Lee, B.M. Hoffman, A.G.M. Barrett, B. Ehrenberg, Photochem. Photobiol. 84 (2008) 764–773.
[7] S. Lee, B.J. Vesper, H. Zong, N.D. Hammer, K.M. Elseth, A.G.M. Barrett, B.M. Hoffman, J.A. Radosevich, Met.-Based Drugs (2008), Article ID 391418.
[8] S. Ristori, A. Salvati, G. Martini, O. Spalla, D. Pietrangeli, A. Rosa, G. Ricciardi, J. Am. Chem. Soc. 129 (2007) 2728–2729.
[9] A. Koca, E. Gonca, A. Gül, J. Electroanal. Chem. 612 (2008) 231–240.
[10] M. Kandaz, A.R. Özkaya, A. Koca, B. Salih, Dyes Pigments 74 (2007) 483–489.
[11] K. Deng, F. Huang, D. Wang, Z. Peng, Y. Zhou, Chem. Lett. 33 (2004) 34–35.
[12] J. Sun, Y. Sun, K. Deng, H. Hou, D. Wang, Chem. Lett. 36 (2007) 586–587.
[13] F. Bonosi, G. Ricciardi, F. Lelj, G. Martini, J. Phys. Chem. 98 (1994) 10613–10620.
[14] B.J. Vesper, K. Salaita, H. Zong, C.A. Mirkin, A.G.M. Barrett, B.M. Hoffman, J. Am. Chem. Soc. 126 (2004) 16653–16658.
[15] P. Sun, H. Zong, K. Salaita, J.B. Ketter, A.G.M. Barrett, B.M. Hoffman, C.A. Mirkin, J. Phys. Chem. B 110 (2006) 18151–18153.
[16] B.E. Smart, J. Fluorine Chem. 109 (2001) 3–11.
[17] C. Isanbor, D. O'Hagan, J. Fluorine Chem. 127 (2006) 303–319.
[18] K.L. Kirk, J. Fluorine Chem. 127 (2006) 1013–1029.
[19] E. Zenkevich, E. Sagun, V. Knyukshto, A. Shulga, A. Mironov, O. Efremova, R. Bonnett, S.P. Songca, M. Kassem, J. Photochem. Photobiol. B 33 (1996) 171–180.
[20] S.K. Pandey, A.L. Gryshuk, A. Graham, K. Ohkubo, S. Fukuzumi, M.P. Dobhal, G. Zheng, Z. Ou, R. Zhan, K.M. Kadish, A. Oseroff, S. Ramaprasad, R.K. Pandey, Tetrahedron 59 (2003) 10059–10073.
[21] I. Kumadaki, A. Ando, M. Omote, J. Fluorine Chem. 109 (2001) 67–81.
[22] T. Goslinski, J. Piskorz, J. Photochem. Photobiol. C 12 (2011) 304–321.
[23] D. Koçak, E. Gonca, J. Fluorine Chem. 131 (2010) 1322–1326.
[24] M. Altunkaya, E. Gonca, Polyhedron 30 (2011) 1035–1039.
[25] H. Akkus, A. Gül, Transit. Met. Chem. 26 (2001) 689–694.
[26] A.H. Cook, R.P. Linstead, J. Chem. Soc. 929 (1937).
[27] S.L.J. Michel, B.M. Hoffman, S.M. Baum, A.G.M. Barrett, Prog. Inorg. Chem. 50 (2001) 473–590.
[28] A. Kalkan, Z.A. Bayir, Monatsh. Chem. 134 (2003) 1555–1560.
[29] S.B. Sesalan, A. Gül, Monatsh. Chem. 131 (2000) 1191–1195.
[30] T.F. Baumann, M.S. Nasir, J.W. Sibert, A.J.P. White, M.M. Olmstead, D.J. Williams, A.G.M. Barrett, B.M. Hoffman, J. Am. Chem. Soc. 118 (1996) 10479–10486.
[31] A. Ogunsipe, D. Maree, T. Nyokong, J. Mol. Struct. 650 (2003) 131–140.
[32] W.F. Law, R.C. Liu, J.H. Jiang, D.K.P. Ng, Inorg. Chim. Acta 256 (1997) 147–150.
[33] D.R. Lide (Ed.), CRC Handbook of Chemistry and Physics, 78th ed., CRC Press LLC, Boca Raton, 1997.
[34] I. Seotsanyana-Mokhosi, N. Kuznetsova, T. Nyokong, J. Photochem. Photobiol. A 140 (2001) 215–222.
[35] T. Goslinski, T. Osmalek, J. Mielcarek, Polyhedron 28 (2009) 3839–3843.
[36] M.P. Cormick, M. Rovera, E.N. Durantini, J. Photochem. Photobiol. A 194 (2008) 220–229.
[37] A. Günsel, M.N. Yaraşir, M. Kandaz, A. Koca, Polyhedron 29 (2010) 3394–3404.
[38] W. Spiller, H. Kliesch, D. Wöhrle, S. Hackbarth, B. Röder, G. Schnurpfeil, J. Porphyrins Phthalocyanines 2 (1998) 145–158.
[39] L.S. Beall, N.S. Mani, A.J.P. White, D.J. Williams, A.G.M. Barrett, B.M. Hoffman, J. Org. Chem. 63 (1998) 5806–5817.
[40] M. Durmuş, V. Ahsen, T. Nyokong, J. Photochem. Photobiol. A 186 (2007) 323–329.
[41] K. Matsumoto, M. Horikoshi, K. Rikimaru, S. Enomoto, J. Oral Pathol. Med. 18 (1989) 498–501.
[42] S.S. Prime, S.V.R. Nixon, S.I.J. Crane, A. Stone, J.B. Matthews, N.J. Maitland, L. Remnant, S.K. Powell, S.M. Game, C. Scully, J. Pathol. 160 (1990) 259–269.
[43] R.D. Fields, M.V. Lancaster, Am. Biotechnol. Lab. 11 (1993) 48–50.
[44] K. Konopka, E. Pretzer, P.L. Felgner, N. Düzgünes, Biochim. Biophys. Acta 1312 (1996) 186–196.